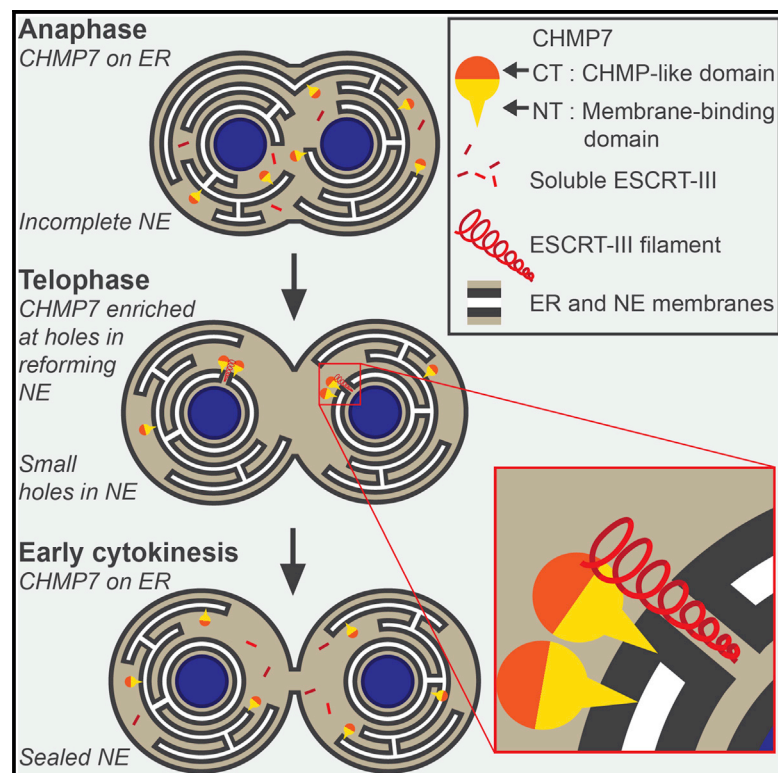


Membrane Binding by CHMP7 Coordinates ESCRT-III-Dependent Nuclear Envelope Reformation

Graphical Abstract



Authors

Yolanda Olmos, Anna Perdrix-Rosell,
Jeremy G. Carlton

Correspondence

jeremy.carlton@kcl.ac.uk

In Brief

ESCRT-III is necessary for closing small holes in the reforming nuclear envelope during mitotic exit. Olmos et al. show that CHMP7, a key component of this machinery, contains a novel membrane-binding domain that is necessary for the assembly of ESCRT-III at this organelle and for the regeneration of a sealed nuclear envelope during mitotic exit.

Highlights

- CHMP7's N terminus is a membrane-binding domain
- Membrane binding allows CHMP7 to localize to the ER
- ER binding is necessary for CHMP7 localization to the reforming NE
- CHMP7's membrane binding is necessary for regeneration of the post-mitotic NE



Membrane Binding by CHMP7 Coordinates ESCRT-III-Dependent Nuclear Envelope Reformation

Yolanda Olmos,¹ Anna Perdrix-Rosell,^{1,2} and Jeremy G. Carlton^{1,3,*}¹Division of Cancer Studies, King's College London, London SE1 1UL, UK²Present address: Tumour-Host Interaction Laboratory, The Francis Crick Institute, Lincoln's Inn Fields Laboratory, London WC2A 3LY, UK³Lead Contact*Correspondence: jeremy.carlton@kcl.ac.uk<http://dx.doi.org/10.1016/j.cub.2016.07.039>

SUMMARY

In addition to its role in membrane abscission during cytokinesis, viral budding, endosomal sorting, and plasma membrane repair [1], the endosomal sorting complex required for transport-III (ESCRT-III) machinery has recently been shown to seal holes in the reforming nuclear envelope (NE) during mitotic exit [2, 3]. ESCRT-III also acts during interphase to repair the NE upon migration-induced rupture [4, 5], highlighting its key role as an orchestrator of membrane integrity at this organelle. While NE localization of ESCRT-III is dependent upon the ESCRT-III component CHMP7 [3], it is unclear how this complex is able to engage nuclear membranes. Here we show that the N terminus of CHMP7 acts as a novel membrane-binding module. This membrane-binding ability allows CHMP7 to bind to the ER, an organelle continuous with the NE, and it provides a platform to direct NE recruitment of ESCRT-III during mitotic exit. CHMP7's N terminus comprises tandem Winged-Helix domains [6], and, by using homology modeling and structure-function analysis, we identify point mutations that disrupt membrane binding and prevent both ER localization of CHMP7 and its subsequent enrichment at the reforming NE. These mutations also prevent assembly of downstream ESCRT-III components at the reforming NE and proper establishment of post-mitotic nucleocytoplasmic compartmentalization. These data identify a novel membrane-binding activity within an ESCRT-III subunit that is essential for post-mitotic nuclear regeneration.

RESULTS AND DISCUSSION

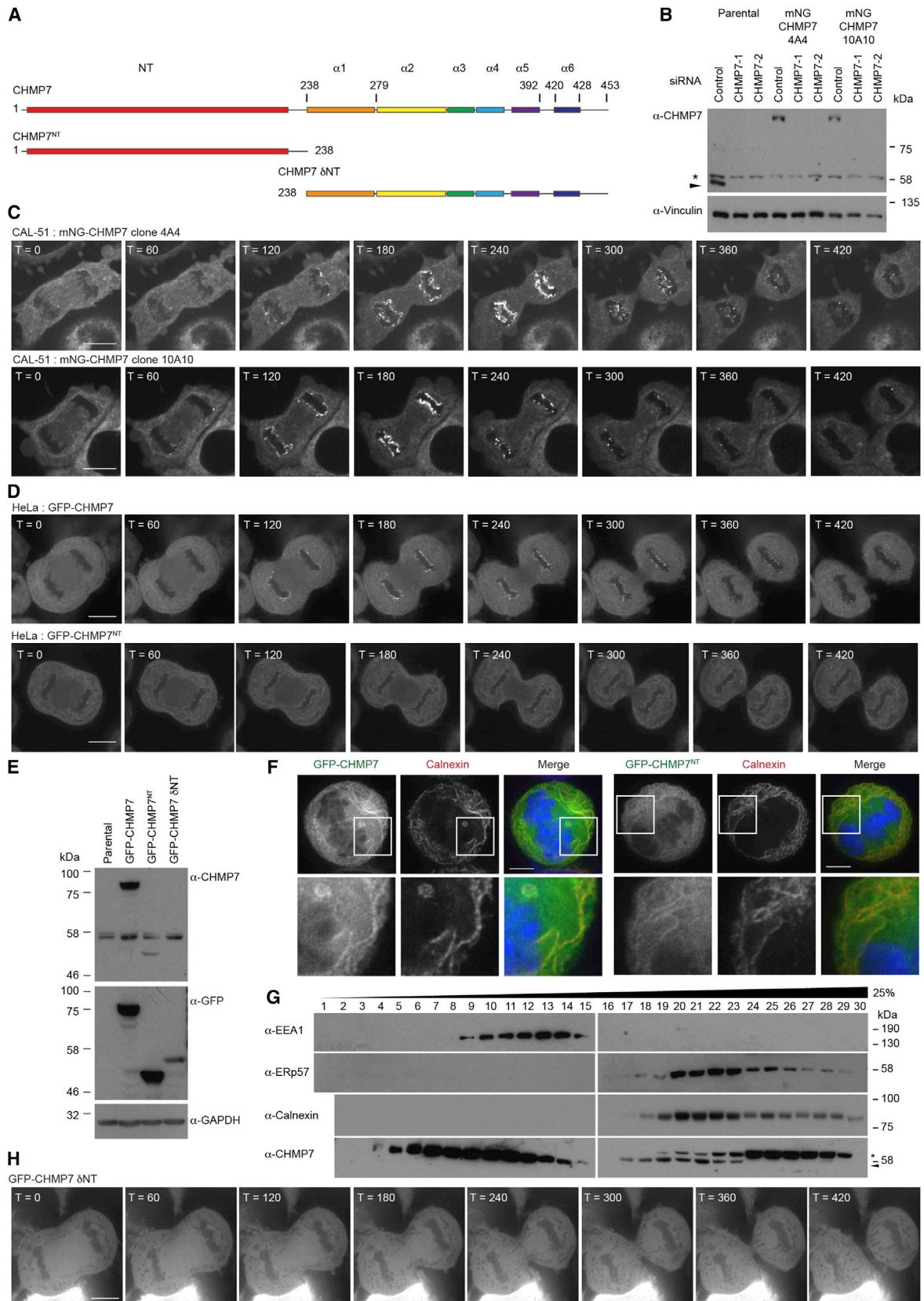
CHMP7 is unique among endosomal sorting complex required for transport-III (ESCRT-III) subunits in that it contains an extended N terminus (NT) (Figures 1A and S1A) that we hypothesized may be important during its role in nuclear envelope (NE) regeneration. Using a dual-nickase CRISPR/Cas9 approach [7], we edited the CHMP7 locus in CAL-51 cells to produce a homozygous N-terminal fusion of monomeric-NeonGreen (mNG) [8] to

CHMP7 under the control of its endogenous promoter (Figures 1B and S1B–S1I). These cells grew normally, suggesting that N-terminal tagging of CHMP7 is benign. We imaged living mNG-CHMP7 cells and found that, while CHMP7 was recruited to the NE during mitotic exit, in addition to a cytoplasmic pool, it decorated ER membranes in interphase and mitotic cells (Figures 1C and S1J; Movie S1). Stably expressed GFP-CHMP7 localized similarly (Figures 1D–1F and S1K–S1M). We saw no localization of GFP-CHMP7 to the midbody (Figure S1N). CHMP7-antisera failed to detect small interfering RNA (siRNA)-sensitive immunofluorescence signal; however, we could detect endogenous CHMP7 in ER fractions from homogenized cells (Figures 1G and S1O).

S. cerevisiae Chm7 was recently shown to localize to the ER [6], suggesting that this localization is evolutionarily conserved. During NE reformation, all other ESCRT-III subunits are recruited from the cytoplasm [2, 3]; given that the NE is formed from the ER [9, 10], a pre-existing ER localization for CHMP7 suggested a platform from which this recruitment could occur. Analysis of HeLa cells stably expressing GFP-CHMP7^{NT} or mCh-CHMP7^{NT} revealed that CHMP7's N terminus directed localization to the ER, but this truncated protein exhibited little stabilization at the reforming NE (Figures 1D and S2A–S2D; Movie S2). In contrast, the C terminus of CHMP7 (GFP-CHMP7 δ NT) was cytosolic and displayed neither ER localization nor stabilization at the reforming NE (Figure 1H; Movie S2), despite containing the CHMP4B/ESCRT-III interaction domain [11]. CHMP7 is responsible for recruiting downstream ESCRT-III components to the reforming NE through CHMP4B. Fusion of siRNA-resistant CHMP7^{NT} to CHMP4B directed cytoplasmic CHMP4B to the mitotic ER and restored its enrichment at sites of annular fusion at the forming NE, in the absence of endogenous CHMP7 (Figures S2E–S2G).

Analysis of the secondary structure of CHMP7^{NT} has revealed the presence of tandem winged helix (WH) domains [6, 12], resembling those found in ESCRT-II subunits (Figure S3A). During endosomal sorting, membrane-anchored ESCRT-II serves to recruit ESCRT-III to endosomes through interaction of the second WH domain of VPS25 with the ESCRT-III component VPS20/CHMP6 [13, 14]. As CHMP7 initiates ESCRT-III assembly at the NE, we wondered whether its N terminus acted as a membrane adaptor at this organelle. HHpred (<https://toolkit.tuebingen.mpg.de/hhpred>) alignments of CHMP7 matched its NT to VPS25 [6], and, by aligning predicted secondary structural elements in CHMP7 to those present in the crystal structure of VPS25, we noted an evolutionarily conserved extension of the





(legend on next page)

loop between the $\beta 2$ - $\beta 3$ hairpin in the first WH domain of CHMP7^{NT} (Figure S3A).

Deletions through CHMP7^{NT} were poorly expressed (Figures S2C and S2D), so we performed scanning mutagenesis through CHMP7^{NT} to identify ER localization determinants (Figures S3B and S3C). We discovered 12 mutagenic tetrads that prevented ER localization, five of which were found on the extended loop in CHMP7^{NT}-WH1. We created a homology model of CHMP7^{NT} (lacking the extended loop) and mapped the remaining mutations to regions that were either in or engaged with residues on the WH1 $\beta 2$ - $\beta 3$ hairpin (Figure S3D). Deletion of this loop (CHMP7 $\delta 107$ -148) prevented ER localization (Figure 2A). In case alanine changes in blocks of four prevented proper folding, we mutated individual residues within this loop to fine-map determinants of ER localization. Mutation of six evolutionarily conserved hydrophobic residues (W118, W121, F126, L127, L128, and L131) or deletion of this hydrophobic stretch ($\delta 118$ -128) prevented ER localization of CHMP7^{NT} (Figures 2A and 2B). These mutations prevented full-length CHMP7 from localizing to the ER and becoming enriched at the reforming NE (Figure 2C; Movie S3).

We wondered whether the hydrophobic residues necessary for ER localization acted as a membrane-binding region to anchor this protein in the ER, and we found that HIS-CHMP7^{NT} and GST-CHMP7^{NT}, but not GST, could be captured upon liposomes (Figures 3A-3D and S4A). The fusogenic lipid diacylglycerol has been implicated in NE reformation [15], however, membrane interaction of CHMP7^{NT} was insensitive to the presence of diacylglycerol (Figures 3C and 3D). We also found membrane interaction to be insensitive to the degree of membrane curvature (Figures S4B and S4C). Mutation of residues that disrupted ER localization prevented membrane binding, with deletion of the hydrophobic cluster ($\delta 118$ -128) or mutation of L127A or L131A having the strongest effect (Figures 3E and 3F). Importantly, these mutations did not destabilize GST-CHMP7^{NT} (Figure S4D).

Consistent with a role for CHMP7 in recruiting CHMP4 proteins to the reforming NE (Figures S2F and S2G) [3], we found that stable expression of siRNA-resistant HA-CHMP7 (HA-CHMP7^R), but neither HA-CHMP7^R $\delta 118$ -128 nor HA-CHMP7^R L127A, could support enrichment of GFP-CHMP4B at the reforming NE in CHMP7-depleted cells (Figures 4A-4C; Movie S4). Further, we found that CHMP7 depletion prevented enrichment of endogenous CHMP2A at the reforming NE (Figures 4D and 4E). Failure to recruit CHMP2A to this organelle leaves holes in the reforming NE [2], and, consistent with this

(and [5]), we found that CHMP7 depletion led to a poorly sealed post-mitotic NE (Figures 4F and 4G). Assembly of CHMP2A at the reforming NE in CHMP7-depleted cells could be rescued by stable expression of HA-CHMP7^R or HA-CHMP7^{NT-R}/CHMP4B, but not by HA-CHMP7^R δ NT, HA-CHMP7^R $\delta 118$ -128, or HA-CHMP7^R L127A (Figures 4H and 4I). Midbody accumulation of endogenous CHMP2A was unaffected in CHMP7-depleted cells expressing HA-CHMP7^R δ NT (Figure 4J), indicating that the membrane-binding ability of CHMP7 is required for NE-specific ESCRT-III function. While the nucleocytoplasmic compartmentalization defect induced by CHMP7 depletion could be rescued by stable expression of HA-CHMP7^R, stable expression of HA-CHMP7^R δ NT, HA-CHMP7^R $\delta 118$ -128, or HA-CHMP7^R L127A failed to rescue this compartmentalization defect (Figure 4K). Just as the chimeric CHMP7^{NT-R}/CHMP4B could support ESCRT-III assembly at the reforming NE, it could rescue the nucleocytoplasmic compartmentalization defect elicited by CHMP7 depletion (Figure 4K).

We describe a membrane-binding domain that localizes CHMP7 to the ER and, given the continuity of the ER with the NE [16], its subsequent function in regenerating a sealed NE during mitotic exit. Consistent with a role for ESCRT-II in recruiting ESCRT-III to cellular membranes [17-19], the ESCRT-II-like N terminus of CHMP7 directs ESCRT-III assembly at the NE. In *C. elegans*, ESCRT-II has been reported to localize to the sarco-plasmic reticulum, suggesting that the tandem WH fold may play a broader role in ER targeting [20]. We identify specific residues in the first WH domain of CHMP7^{NT} domain that are necessary for membrane binding, ER localization, subsequent enrichment of CHMP7 at the reforming NE, and, given CHMP7's ability to bind CHMP4 proteins [6, 11], that are essential for the assembly of downstream ESCRT-III components and for ESCRT-III-dependent NE regeneration. In the absence of membrane-bound CHMP7, ESCRT-III cannot assemble at the NE. CHMP7^{NT} was not stabilized at the reforming NE, suggesting that subsequent engagement of ESCRT-III [11] (and ESCRT-III-binding partners such as Spastin [3] or UFD1L [2]) by the C terminus of CHMP7 provides a stabilizing cue.

Recent reports describing the association of CHMP7's C terminus with LEM family proteins [21] and that LEMD2 depletion impairs ESCRT-III assembly at this organelle [22] indicate that these also may be candidates that regulate the enrichment of CHMP7 at sites of annular fusion. While CHMP7's membrane binding was curvature insensitive, a geometric constraint of the narrow-radius hole that is to be closed also may restrict

Figure 1. CHMP7 Is an ER-Localized Protein that Is Enriched at the NE during Mitotic Exit

(A) Schematic depicting constructs used in this study.

(B and C) CAL-51 cells edited to express mNG-CHMP7 were resolved and examined by western blotting with anti-CHMP7 and anti-Vinculin (B) or imaged live (C). In this and all other figures, endogenous CHMP7 is marked by an arrowhead (*, non-specific band).

(D-F) HeLa cells stably expressing GFP-CHMP7 and GFP-CHMP7^{NT} were imaged live (D), lysed, resolved, and examined by western blotting with anti-GFP, anti-CHMP7, or anti-GAPDH antisera (E) or fixed and stained with anti-Calnexin and DAPI (F). Images in (D) are representative of all cells imaged and 22/22 (GFP-CHMP7) and 21/21 (GFP-CHMP7^{NT}) captured movies. Co-localization of GFP-CHMP7 and GFP-CHMP7^{NT} with Calnexin was observed in 7/7 and 13/13 scored cells, respectively.

(G) Post-nuclear supernatants from Cos7 cells were fractionated through a continuous iodixanol gradient and analyzed by western blotting with the indicated antisera.

(H) HeLa cells stably expressing GFP-CHMP7 δ NT were imaged live. Images are representative of all cells imaged and 5/5 captured movies. Time interval is presented in seconds post-cortical ingression.

In all micrographs, the scale bar represents 10 μ m. See also Figure S1.

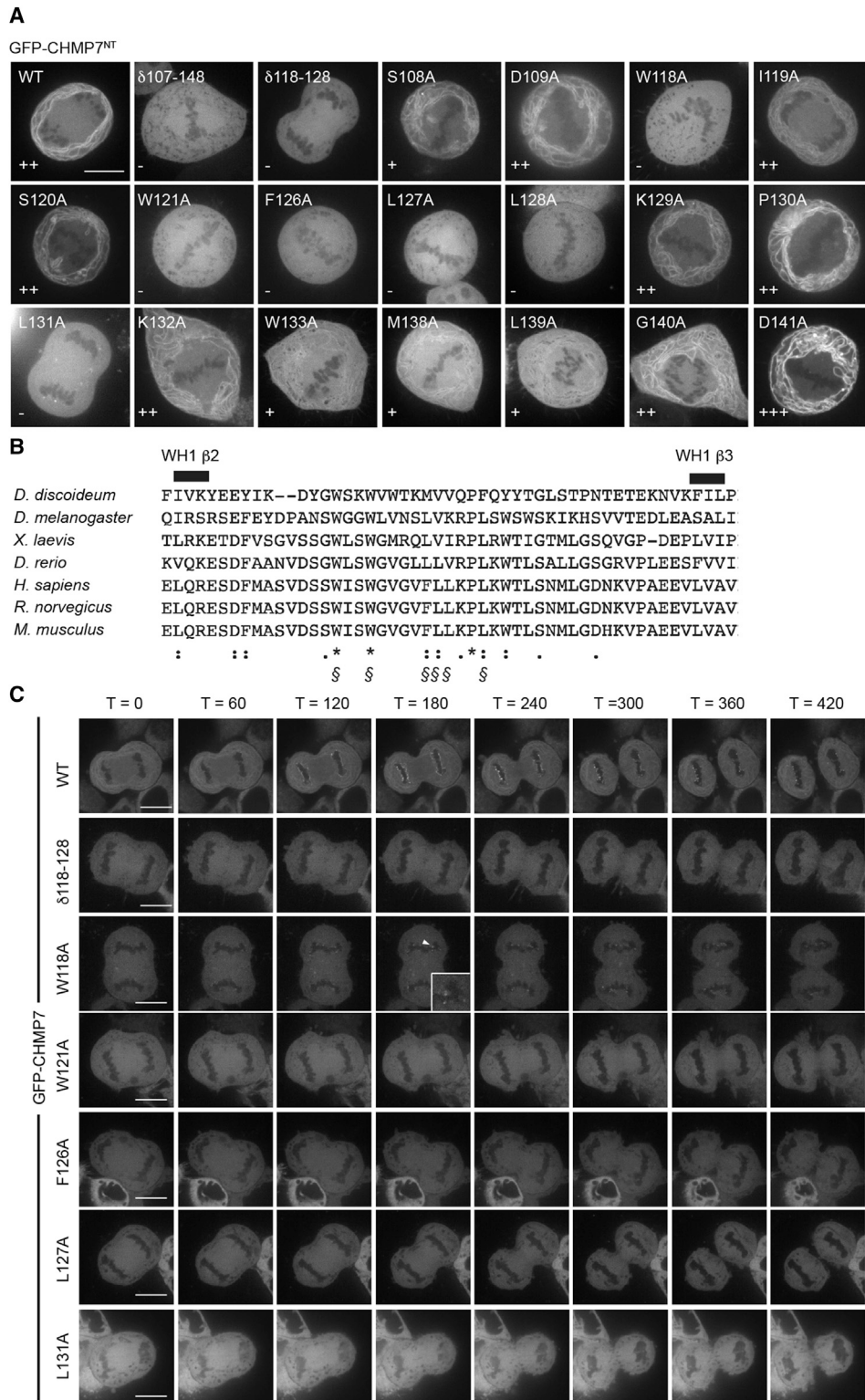


Figure 2. Mapping Activities in CHMP7^{NT} that Govern ER Localization

(A) HeLa cells were transfected with the indicated GFP-CHMP7^{NT} plasmids and imaged live; individual residues within the β2-β3 insertion that disrupted ER localization when previously mutated in blocks of four (Figures S3B–S3D) were mutated to alanine. Reticular localization is indicated as follows: –, none/cytoplasmic; +, reduced; ++, normal; and +++, enhanced). Reticular localization was observed in the indicated number of captured images from three independent experiments. NT, 11/11; Δ107–148, 0/11; Δ118–128, 0/13; S108A, 12/12; D109A, 11/11; W118A, 0/13; I119A, 11/11; S120A, 11/11; W121A,

(legend continued on next page)

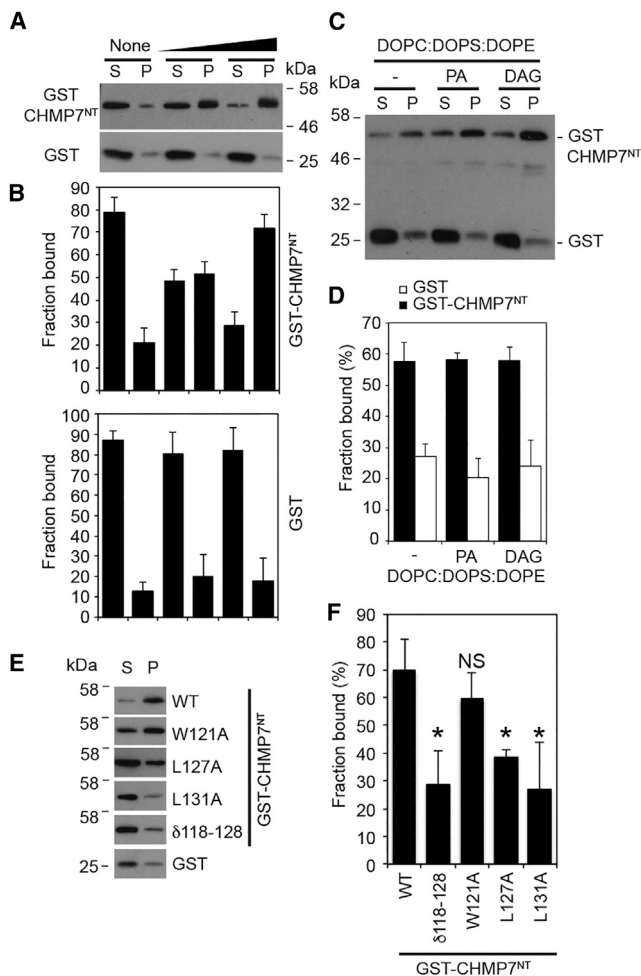


Figure 3. CHMP7^{NT} Binds Lipid Membranes

GST or GST-CHMP7^{NT} was incubated for 5 min (A and B) or 15 min (C–F) with Folch (A, B, E, and F) or synthetic (C and D; 60% 1,2-dioleoyl-*sn*-glycero-3-phosphocholine [DOPC], 20% 1,2-dioleoyl-*sn*-glycero-3-phosphoserine [DOPS], and 20% 1,2-dioleoyl-*sn*-glycero-3-phosphoethanolamine [DOPE]) liposomes. In (A), increasing amounts (0, 10, or 50 μg) of liposomes were added. In (D), 2.5% 1,2-dioleoyl-*sn*-glycerol (DAG) or 1,2-dioleoyl-*sn*-glycero-3-phosphate (PA) was added, as indicated. Liposomes were collected by ultracentrifugation. Pelleted (P) and soluble (S) fractions were resolved and analyzed by western blotting with anti-GST antisera. Western blots from (A), (C), and (E) were quantified by densitometry (mean ± SD) (B and D, N = 3; F, WT, N = 7; δ118–128, N = 7; W121A, N = 7, NS; L127A, N = 4; L131A, N = 4). Statistical significance was calculated using one-way ANOVA with Dunnett's multiple comparison test (*p < 0.0001). See also Figure S4.

subsequent ESCRT-III assembly to these sites. This geometric constraint may allow for a critical concentration of ESCRT-III components to be reached for productive filament assembly at

the NE rather than the ER. CHMP7 is thus an ER-specific membrane adaptor for ESCRT-III that provides an activity essential for post-mitotic organelle biogenesis, and it may be necessary for repair of the NE under physiological and pathological conditions, such as in cancer or during migration-induced rupture [4, 5, 23].

SUPPLEMENTAL INFORMATION

Supplemental Information includes Supplemental Experimental Procedures, four figures, and four movies and can be found with this article online at <http://dx.doi.org/10.1016/j.cub.2016.07.039>.

AUTHOR CONTRIBUTIONS

J.G.C. conceived and designed the study. J.G.C., A.P.-R., and Y.O. performed data acquisition, analysis, and interpretation. J.G.C. and Y.O. drafted and revised the manuscript.

ACKNOWLEDGMENTS

J.G.C. is a Wellcome Trust Research Career Development Fellow (093603/Z/10/Z). We acknowledge the Nikon Imaging Centre at KCL and the Programme in Infection and Immunity Flow Cytometry Core at KCL for access to equipment. We thank Camille Wouters and Nisreen Chahid who assisted with cloning as part of high school Nuffield Research Placements. We thank Dr. Pierfrancesco Marra (KCL) for guidance on density-gradient centrifugation.

Received: April 29, 2016

Revised: June 25, 2016

Accepted: July 15, 2016

Published: September 8, 2016

REFERENCES

- Hurley, J.H. (2015). ESCRTs are everywhere. *EMBO J.* 34, 2398–2407.
- Olmos, Y., Hodgson, L., Mantell, J., Verkade, P., and Carlton, J.G. (2015). ESCRT-III controls nuclear envelope reformation. *Nature* 522, 236–239.
- Vietri, M., Schink, K.O., Campsteijn, C., Wegner, C.S., Schultz, S.W., Christ, L., Thoresen, S.B., Brech, A., Raiborg, C., and Stenmark, H. (2015). Spastin and ESCRT-III coordinate mitotic spindle disassembly and nuclear envelope sealing. *Nature* 522, 231–235.
- Raab, M., Gentili, M., de Bely, H., Thiam, H.R., Vargas, P., Jimenez, A.J., Lautenschlaeger, F., Voituriez, R., Lennon-Duménil, A.M., Manel, N., and Piel, M. (2016). ESCRT III repairs nuclear envelope ruptures during cell migration to limit DNA damage and cell death. *Science* 352, 359–362.
- Denais, C.M., Gilbert, R.M., Isermann, P., McGregor, A.L., te Lindert, M., Weigel, B., Davidson, P.M., Friedl, P., Wolf, K., and Lammerding, J. (2016). Nuclear envelope rupture and repair during cancer cell migration. *Science* 352, 353–358.
- Bauer, I., Brune, T., Preiss, R., and Kölling, R. (2015). Evidence for a non-endosomal function of the *Saccharomyces cerevisiae* ESCRT-III-like protein Chm7. *Genetics* 201, 1439–1452.
- Cong, L., Ran, F.A., Cox, D., Lin, S., Barretto, R., Habib, N., Hsu, P.D., Wu, X., Jiang, W., Marraffini, L.A., and Zhang, F. (2013). Multiplex genome engineering using CRISPR/Cas systems. *Science* 339, 819–823.

0/12; F126A, 0/12; L127A, 0/14; L128A, 0/14; K129A, 13/13; P130A, 13/13; L131A, 0/12; K132A, 12/13; W133A, 13/14; M138A, 15/15; L139A, 11/12; G140A, 16/16; D141A, 13/13.

(B) Sequence alignment of the insertion between β2 and β3 in the CHMP7^{NT} WH1 domain from the indicated organisms. Conservation extent is as follows: *, complete; :, strongly similar; +, weakly similar; §, residues necessary for ER localization.

(C) HeLa cells expressing the indicated GFP-CHMP7 constructs were imaged live (time in seconds post-cortical ingression). Images are representative of 3/3 acquired movies and 50/50 scored cells per mutation. Limited enrichment on the telophase NE (boxed) was observed for GFP-CHMP7 W118A, suggesting that some degree of ER localization persists in this case.

In all micrographs, the scale bar represents 10 μm. See also Figures S2 and S3.

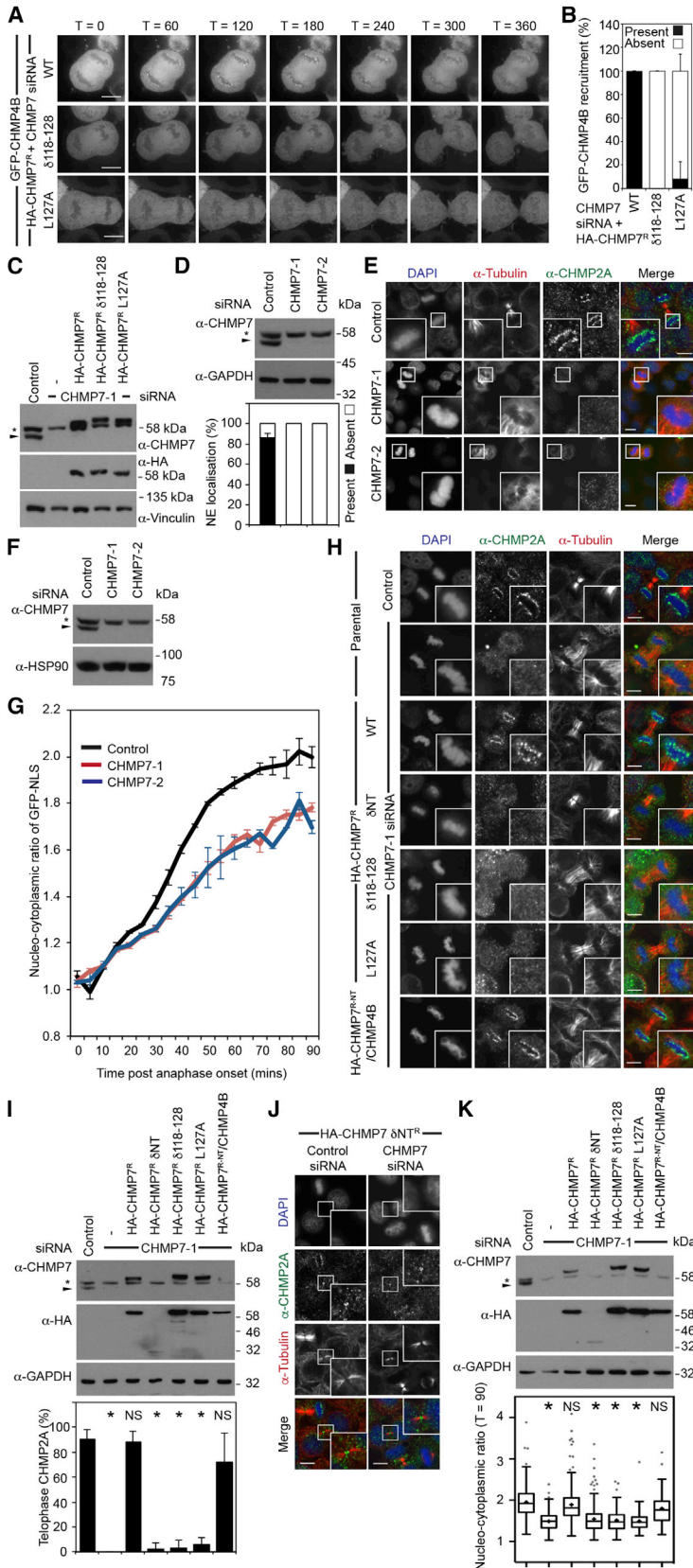


Figure 4. Membrane Binding by CHMP7 Is Essential for ESCRT-III-Dependent NE Reformation during Mitotic Exit

(A) siRNA-transfected HeLa cells stably expressing both GFP-CHMP4B and the indicated HA-CHMP7^R proteins were imaged live (time interval in seconds).

(B) Quantification of NE enrichment of GFP-CHMP4B from (A) (mean \pm SD; CHMP7 siRNA + HA-CHMP7^R, 23/23, N = 4; CHMP7 siRNA and HA-CHMP7^R $\delta 118-128$, 0/15, N = 3; CHMP7 siRNA and HA-CHMP7^R L127A, 1/16, N = 3).

(C) Resolved lysates of cells from (A) were examined by western blotting with anti-CHMP7, anti-HA, or anti-Vinculin.

(D and E) siRNA-transfected HeLa cells were fixed; stained with anti-tubulin, anti-CHMP2A, and DAPI; and examined by immunofluorescence (E) or resolved and examined by western blotting with anti-CHMP7 or anti-GAPDH (D). Assembly of CHMP2A at the telophase NE was quantified (D, mean \pm SD; n = 40, N = 2; p = 0.0008, calculated by two-tailed Student's t test).

(F and G) siRNA-transfected HeLa cells stably expressing GFP-NLS and H2B-mCh were analyzed by western blotting with anti-CHMP7 and anti-HSP90 (F) or were imaged live and the degree of nucleocytoplasmic compartmentalization was calculated at the indicated time points (G, Mean \pm SEM; control, N = 4, n = 40; CHMP7 siRNA-1, N = 3, p = 0.010, n = 28; CHMP7 siRNA-2, N = 3, n = 28, p = 0.003). Significance was calculated after 90 min using one-way ANOVA with Dunnett's multiple comparison test.

(H and I) HeLa cells stably expressing the indicated HA-tagged, siRNA-resistant CHMP7 proteins were transfected with control or CHMP7-targeting siRNA and fixed; stained with anti-tubulin, anti-CHMP2A, and DAPI; and examined by immunofluorescence (H) or resolved and analyzed by western blotting with anti-CHMP7, anti-HA, and anti-GAPDH (I). Cells from (H) were quantified (I, mean \pm SD; control, N = 5, n = 80; CHMP7 siRNA, N = 4, n = 34, p < 0.001; CHMP7 siRNA and HA-CHMP7^R, N = 4, n = 52, not significant [NS, p = 0.995]; CHMP7 siRNA and HA-CHMP7^R δ NT, N = 4, n = 40, p < 0.001; CHMP7 siRNA and HA-CHMP7^R $\delta 118-128$, N = 3, n = 30, p < 0.001; CHMP7 siRNA and HA-CHMP7^R L127A, N = 3, n = 32, p < 0.001; CHMP7 siRNA and HA-CHMP7^RNT/CHMP4B, N = 3, n = 31, NS [p = 0.055]). Significance was calculated using one-way ANOVA with Dunnett's multiple comparison test (*, significant).

(J) HeLa cells stably expressing HA-CHMP7^R δ NT were transfected with control or CHMP7-targeting siRNA; fixed; stained with anti-tubulin, anti-CHMP2A, and DAPI; and examined by immunofluorescence. Midbody localization of CHMP2A was observed in 30/30 cases (Ctrl) and 29/30 cases (CHMP7 siRNA) (N = 3).

(K) siRNA-transfected HeLa cells stably expressing GFP-NLS, H2B-mCh, and the indicated HA-tagged siRNA-resistant CHMP7 proteins were examined by western blotting with anti-CHMP7, anti-HA, or anti-GAPDH or were imaged live and the degree of nucleocytoplasmic compartmentalization was calculated 90 min post-anaphase onset (mean \pm SEM; control, 1.93 \pm 0.04, N = 9, n = 236; CHMP7 siRNA, 1.51 \pm 0.03, N = 9, n = 252, p < 0.0001; CHMP7 siRNA and HA-CHMP7^R, 1.88 \pm 0.05, N = 8, n = 257, NS [p = 0.8909]; CHMP7 siRNA and HA-CHMP7^R δ NT, 1.54 \pm 0.08, N = 4, n = 207, p = < 0.0001; CHMP7 siRNA and HA-CHMP7^R $\delta 118-128$, 1.53 \pm 0.1, N = 3, n = 101, p = 0.0003; CHMP7 siRNA and HA-CHMP7^R L127A, 1.50 \pm 0.08, N = 3, n = 101, p = 0.0001; CHMP7 siRNA and HA-CHMP7^RNT/CHMP4B, 1.73 \pm 0.1, N = 3, n = 76, NS [p = 0.1556]). Statistical significance was calculated using one-way ANOVA with Dunnett's multiple comparison test from experimental means (N); *, significant. Tukey whiskers and mean (+) are displayed.

In all micrographs, the scale bar represents 10 μ m.

8. Shaner, N.C., Lambert, G.G., Chammas, A., Ni, Y., Cranfill, P.J., Baird, M.A., Sell, B.R., Allen, J.R., Day, R.N., Israelsson, M., et al. (2013). A bright monomeric green fluorescent protein derived from *Branchiostoma lanceolatum*. *Nat. Methods* *10*, 407–409.
9. Lu, L., Ladinsky, M.S., and Kirchhausen, T. (2009). Cisternal organization of the endoplasmic reticulum during mitosis. *Mol. Biol. Cell* *20*, 3471–3480.
10. Anderson, D.J., and Hetzer, M.W. (2007). Nuclear envelope formation by chromatin-mediated reorganization of the endoplasmic reticulum. *Nat. Cell Biol.* *9*, 1160–1166.
11. Horii, M., Shibata, H., Kobayashi, R., Katoh, K., Yorikawa, C., Yasuda, J., and Maki, M. (2006). CHMP7, a novel ESCRT-III-related protein, associates with CHMP4b and functions in the endosomal sorting pathway. *Biochem. J.* *400*, 23–32.
12. Sundquist, W.I., and Ullman, K.S. (2015). CELL BIOLOGY. An ESCRT to seal the envelope. *Science* *348*, 1314–1315.
13. Teis, D., Saksena, S., Judson, B.L., and Emr, S.D. (2010). ESCRT-II coordinates the assembly of ESCRT-III filaments for cargo sorting and multivesicular body vesicle formation. *EMBO J.* *29*, 871–883.
14. Im, Y.J., Wollert, T., Boura, E., and Hurley, J.H. (2009). Structure and function of the ESCRT-II-III interface in multivesicular body biogenesis. *Dev. Cell* *17*, 234–243.
15. Domart, M.-C., Hobday, T.M.C., Peddie, C.J., Chung, G.H.C., Wang, A., Yeh, K., Jethwa, N., Zhang, Q., Wakelam, M.J.O., Woscholski, R., et al. (2012). Acute manipulation of diacylglycerol reveals roles in nuclear envelope assembly & endoplasmic reticulum morphology. *PLoS ONE* *7*, e51150.
16. Burke, B., and Ellenberg, J. (2002). Remodelling the walls of the nucleus. *Nat. Rev. Mol. Cell Biol.* *3*, 487–497.
17. Im, Y.J., and Hurley, J.H. (2008). Integrated structural model and membrane targeting mechanism of the human ESCRT-II complex. *Dev. Cell* *14*, 902–913.
18. Teo, H., Perisic, O., González, B., and Williams, R.L. (2004). ESCRT-II, an endosome-associated complex required for protein sorting: crystal structure and interactions with ESCRT-III and membranes. *Dev. Cell* *7*, 559–569.
19. Henne, W.M., Buchkovich, N.J., Zhao, Y., and Emr, S.D. (2012). The endosomal sorting complex ESCRT-II mediates the assembly and architecture of ESCRT-III helices. *Cell* *151*, 356–371.
20. Lefebvre, C., Largeau, C., Michelet, X., Fourrage, C., Maniere, X., Matic, I., Legouis, R., and Culetto, E. (2016). The ESCRT-II proteins are involved in shaping the sarcoplasmic reticulum in *C. elegans*. *J. Cell Sci.* *129*, 1490–1499.
21. Webster, B.M., Thaller, D.J., Jaeger, J., Ochmann, S.E., and Lusk, C.P. (2016). Chm7 and Heh1 form a nuclear envelope subdomain for nuclear pore complex quality control. *bioRxiv*. <http://dx.doi.org/10.1101/049148>.
22. Gu, M., Chen, O.S., Lajoie, D., Ladinsky, M.S., Redd, M.J., Nikolova, L., Bjorkman, P.J., Ullman, K.S., Sundquist, W.I., and Frost, A. (2016). LEM2 and CHMP7 function in ESCRT-dependent nuclear envelope closure in yeast and human cells. *bioRxiv*. <http://dx.doi.org/10.1101/049312>.
23. Vargas, J.D., Hatch, E.M., Anderson, D.J., and Hetzer, M.W. (2012). Transient nuclear envelope rupturing during interphase in human cancer cells. *Nucleus* *3*, 88–100.